Analysis of r.c. bridge columns under imposed deformations

Autor(en): **Hellesland, Jostein / Scordelis, Alex C.**

Objekttyp: **Article**

Zeitschrift: **IABSE reports of the working commissions = Rapports des commissions de travail AIPC = IVBH Berichte der Arbeitskommissionen**

Band (Jahr): **34 (1981)**

PDF erstellt am: **02.05.2024**

Persistenter Link: https://doi.org/10.5169/seals-26914

Analysis of R.C. Bridge Columns under Imposed Deformations

Analyse de piles de pont en béton armé sous déformations imposées

Berechnung von Stahlbetonstützen unter aufgezwungenen Verformungen

JOSTEIN HELLESLAND[1]
Visiting Research Engineer
University of California
Berkeley, USA

ALEX C. SCORDELIS
Professor of Civil Engineering
University of California
Berkeley, USA

SUMMARY
A study of reinforced concrete columns under imposed end rotations and displacements is presented. Numerical solutions are obtained using a finite element computer program, PCFRAME, capable of performing nonlinear and time dependent analyses of reinforced and prestressed concrete frames Choice of element subdivision, nonlinear geometric effects, initially applied rotations and time dependent displacements are found to have significant effects on total displacement capacities.

RÉSUMÉ
Est présentée une étude de piles en béton armé sous l'effet de rotations et déplacements imposés aux extrémités. Les solutions sont obtenues en utilisant un programme aux éléments finis, PCFRAME, capable de calculer des structures en béton armé ou précontraint dans une analyse de type non-linéaire et dépendant du temps. Le choix de la décomposition des éléments, des effets du second ordre, des rotations appliquées initialement et des déplacements dépendant du temps se révèlent avoir des effets significatifs sur la capacité de la structure à résister aux déplacements donnés.

ZUSAMMENFASSUNG
Eine Untersuchung an Stahlbetonstützen unter aufgezwungenen Endrotationen und Stützenkopfverschiebungen is dargestellt. Das Finite-Elemente-Computerprogramm PCFRAME, das die nichtlineare Berechnung von Stahlbeton- und Spannbetonrahmen ermöglicht, wurde zur numerischen Auswertung verwendet. Es wird gezeigt, dass die Gesamtverschiebungskapazität der Stützen bedeutend von der Wahl der Elementeinteilung, den nichtlinearen geometrischen Effekten und von den aufgebrachten Vorverformungen, wie z.B. Rotationen und zeitabhängigen Horizontalverschiebungen, beeinflusst wird.

[1] On leave from Dr. Ing. A. Aas-Jakobsen A/S, Oslo Norway.

1. INTRODUCTION

A number of rigorous analytical procedures based on the finite element method have been developed in recent years that are capable of tracing the response of complex structures to varied loadings. One such procedure, developed by Kang and Scordelis [1], has been applied in the present study to examine the non-linear structural response of reinforced concrete columns, as found in bridges and other frame structures, due to imposed deformations.

Imposed deformations in columns are usually caused by relative lateral, Fig. 1a, movements of the column ends arising from length changes of the connecting girders due to prestressing, causing both short and long term (creep) deformations, shrinkage, and temperature changes. Also, girder rotations at the top of bridge columns, Fig. 1b, caused mainly by traffic loading, can generally be treated as imposed deformations on the columns since the superstructure girder usually has a much larger stiffness than the columns.

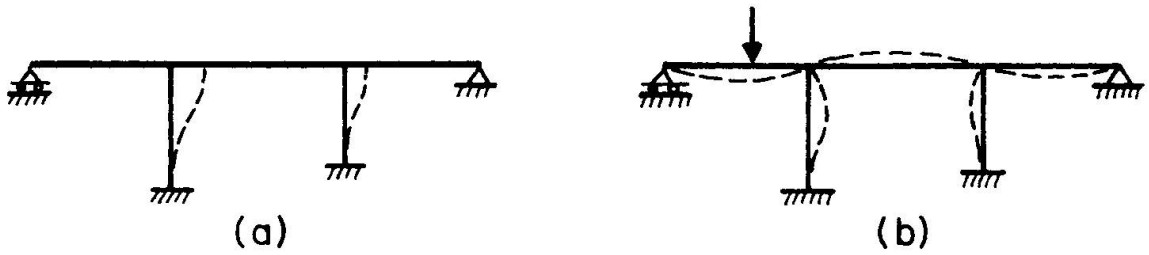

Fig. 1 Imposed Deformations in Bridge Columns

In the usual strength analysis the problem is generally that of determining the largest load the structure can carry. However, the problem in a pure imposed or controlled deformation analysis, in which the structure primarily must accommodate given rotations or displacements rather than carry loads, the problem is generally that of determining the maximum deformation the structure can be subjected to.

Imposed deformation studies of beams have been mainly related to short and long term settlements of supports and deal mainly with the linear [2] and the pre-yielding ranges [3]. Previous nonlinear studies of short and slender columns have been limited to short term end displacement aspects [4].

The main objectives of the present study are to determine end rotation and end displacement capacities of short and slender columns considering both single and combined action, and to study the effect of long term displacements and column creep on displacement capacities. The finite element analysis used for this purpose [1] takes both nonlinear material and geometric effects, i.e., the effects of axial loads on deflections, as well as time dependent concrete properties into account. Pure flexural solutions are sought, thus neglecting spread of inelastic zones due to extended concrete crushing, bond slip, inclined shear cracking, etc. Effects of element subdivision on such results are discussed. A comparison of theoretical predictions with test data is also presented.

Detailed results of the present investigation are given in [5], where the effect of previously imposed deformations on lateral load capacities of unbraced frames also has been studied. However, this aspect is not discussed herein.

2. METHOD OF ANALYSIS

The method of analysis employed in the present study is described in detail elsewhere [1,6]. Thus, only a brief review is given below.

2.1 Analytical Model and Solution Procedure

The analysis is based on the incremental form of the displacement formulation of the finite element method. Equilibrium equations for the total structure are set up and solved in a global coordinate system, which is fixed in space. The direct stiffness method is used to form the structure stiffness matrix.

The structure is divided into straight, one dimensional beam elements with the usual three degrees of freedom at each end, Fig. 2., and with the standard linear and cubic Hermitian shape functions describing the axial and transverse displacements between ends. Shearing deformations are not considered. The origin and direction of the local Cartesian coordinate system passing through the ends of the element, Fig. 2, follow the element, which is considered to be in a continuous quasi-static motion. Nonlinear geometric effects are accounted for by continuously updating the nodal point geometry and the transformation matrix between local and global coordinates.

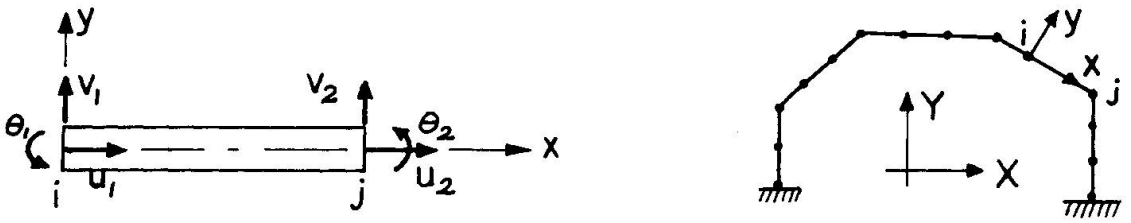

Fig. 2 Beam Element and Frame Structure

Different cross sections, symmetric about the local y-axis, but otherwise of arbitrary shape, and different material properties may be assigned to each element. Cross sections may be reinforced with both ordinary and prestressing steel, applied either in the pretensioned or post-tensioned sense. Cross sections are divided into a finite number of concrete and steel layers, each of which is assumed to be under uniaxial strain. Navier's plane section hypothesis is assumed to govern the distribution of total strains across sections. No bond slip is assumed to take place between rebars and concrete. Nonlinear material properties including cracking of the concrete are considered.

Time dependent load history and time dependent effects of material properties are considered using a step forward integration approach by dividing the time domain into a finite number of intervals of constant or varying length. External loads and equivalent loads due to nonmechanical strains (creep etc.) are applied in a specified number of load steps at each time step.

The nonlinear equilibrium equations are solved by an unbalanced load iteration method for each load step. Internal resisting loads are evaluated numerically by a 3-point Gaussian Quadrature over the current length of the element combined with a mid-point layer integration over the cross section. Stiffness matrices are evaluated at the center of each element only. Incremental solutions for each load step are added to previous totals to arrive at the current updated solution. In this manner, the structural response can be traced through the elastic, cracked, inelastic and ultimate ranges.

2.2 Material Properties

The total concrete strain ε at a given time and point in the structure is taken as the direct sum of mechanical (or instantaneous) strains ε_c and non-mechanical strains due to creep, shrinkage, aging and thermal effects. Incremental strains due to cyclic or repeated loading are not considered.

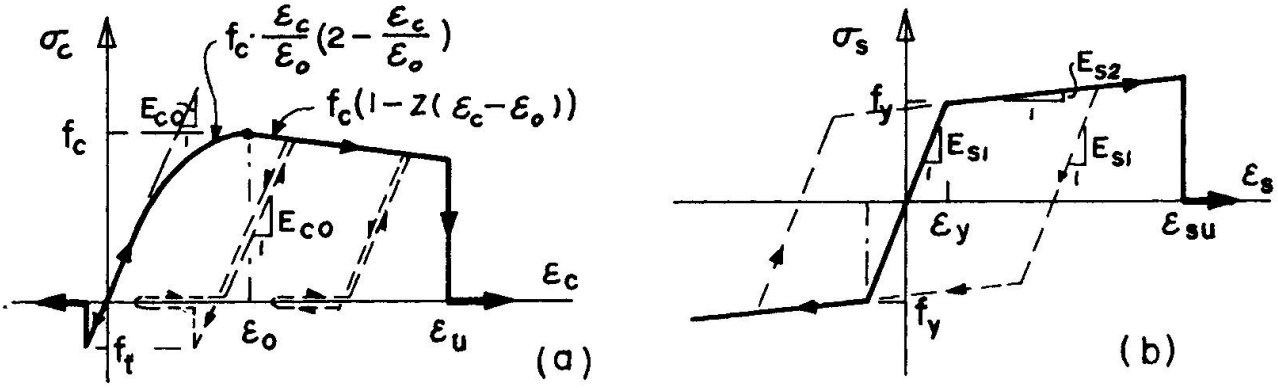

Fig. 3 Stress-Strain Relationships for Concrete (a) and Reinforcing Steel (b)

The nonlinear constitutive stress-strain relationships governing the response of the individual concrete and steel layers are shown in Fig. 3. The monotonic stress-strain curves are taken as envelope curves for the assumed nondegrading unloading-reloading response. Where the concrete tensile stress in a layer exceeds a specified tensile strength, f_t, cracking is assumed to occur. Once cracked, concrete can not again take tensile stress. The structural concrete compressive strength, f_c, taken as a function of the cylinder strength, f'_c, may vary with time.

Creep strain $\varepsilon_{cc}(t)$ of concrete is evaluated by an age and temperature dependent formulation based on the method of superposition. Thus,

$$\varepsilon_{cc}(t) = \int_0^t c\left(t', t-t', T\right) \frac{\partial \sigma(t')}{\partial t'} \tag{1}$$

$$c\left(t', t-t', T\right) = c_u(t') \sum_{i=1}^{m} a_i \left[1 - e^{-\phi(T)(t-t')/\tau_i}\right] \tag{2}$$

The creep compliance function, or specific creep $c(t',t-t',T)$, is the creep at time t' with temperature T. The values a_i (adding up to unity) and τ_i are constants selected to fit experimental or empirical data. $c_u(t')$ is the ultimate specific creep, which is a function of t', and $\phi(T)$ is a "temperature shift function". Temperaure effects on creep will not be considered in the present study. Consequently, $\phi(T)$ will be set equal to unity. Nonlinear creep effects at higher stress levels may be accounted for by replacing the actual stress by an "effective stress" according to specified input parameters.

2.3 Computer Program

The numerical solution described above for geometric, material and time dependent nonlinear analysis of reinforced or prestressed concrete planar frames has been incorporated into a computer program PCFRAME [6].

The input consists of: structure geometry and boundary conditions; element cross section and material properties; load history; time dependent properties and convergence tolerances.

The output, which can be requested for each iteration or each load increment at each time step, consists of the following: (1) joint displacements and rotations; (2) support reaction forces and moments; (3) unbalanced loads and moments; (4) element forces and moments (moments at the two end joints and the axial force); and (5) stresses, strains, and the material states on the stress-strain curve for each concrete and reinforcing steel layer and prestressing steel segment.

The computer program was used to obtain the numerical results described in the following sections.

3. EFFECT OF ELEMENT SUBDIVISION (MESH SIZE)

In linear elastic analyses, the finite element displacement method gives lower bound solutions for displacements. This may not be so for inelastic analyses. In order to study the effect of element subdivision, analyses of a symmetrically reinforced concrete cantilever column, Fig. 4, subject to constant axial load and increasing lateral displacement at the free end, were carried out for several element subdivisions, two of which are discussed below.

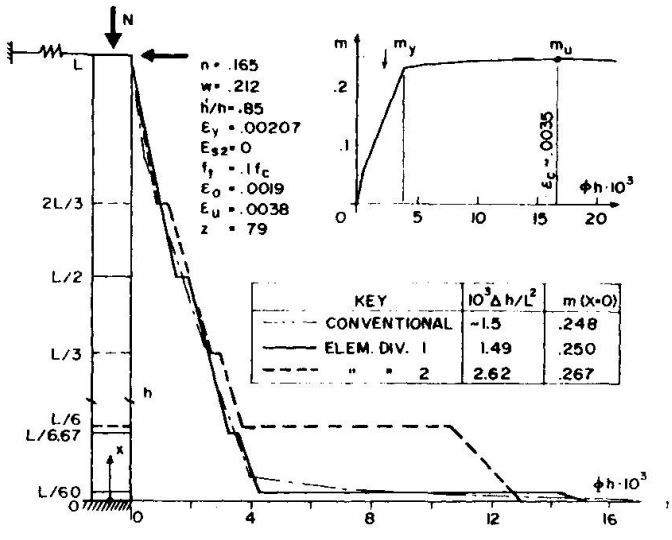

Fig. 4 Curvatures, Top Displacements and Base Moments for Different Element Subdivisions (First Order Analysis)

Element subdivisions "1" (full line) and "2" (broken line), material and section properties are given in Fig. 4. Elastic-perfectly plastic stress-strain properties are assumed for the rebars, and the concrete cross sections are divided into 20 equal layers. The sectional moment-curvature relationship, computed in conventional manner based on the monotonic stress-strain curves, is shown in the upper right hand corner of Fig. 4. It becomes very flat following yielding of the tensile steel, and is typical for low axial load levels. The axial load in the present analysis ($n = N/f_c bh = 0.165$) is 35% of the so-called "balanced" load. Maximum moment resistance M_u occurs in this case for a maximum concrete compressive strain of approximately 0.0035.

From a design point of view, it is of interest to compare finite element incremental load results with results based on conventional sectional M-ϕ considerations, corresponding to the above maximum concrete compressive strain (0.0035) at the column base.

Curvature distributions along the column length, displacements at the free end (Δ) and moments at the base ($m = M/f_c bh^2$) are given in Fig. 4. Geometric nonlinear effects are negligible, and are ignored in this example. Thus, the external moment distribution is linear. The "conventional" top displacement is obtained by a semigraphical integration of curvatures.

Element subdivision "1", with an element length of L/60 at the base, or approximately 1/3 of the conventional flexural plastic hinge length ($L_p = L(M_u-M_y)/M_u \simeq L/17.5$) gives results in satisfactory agreement with the conventional analysis, while element subdivision "2", where the shortest element at the base extends well into the elastic zone, overestimates displacement and moment by approximately 75% and 8% respectively.

As constrained by the assumed beam displacement functions used in the finite element analysis, which are exact for ideal elastic materials, the curvature distribution becomes linear within each element, and, due to the change in stiffness as cracking occurs, discontinuous at element nodes even in the pre-yield range. However, the results are not very sensitive to the size of elements entirely in the pre-yield range. If curvatures in the inelastic region as such were of interest, rather than displacements, a finer division using several small elements over the flexural plastic hinge length would be required.

With increasing constant axial load level, the stiffness will be reduced more gradually with increasing curvature, and also, the curvature corresponding to M_u will become smaller. The errors due to a coarse element subdivision in the inelastic region will thus be smaller than in the case considered above.

In a real structure, the inelastic deformations are usually larger than those predicted by the pure flexural hinge, as actual failure is spread over a finite zone rather than at a single section, due to such factors as spread of crushing, bond slip, etc., and also due to diagonal shear cracking in short, stiff members. Thus, a coarse element at the critical region, such as "2" in Fig. 4, which in a physical sense have extended the inelastic zone to the full length of the first element, might actually give displacements in better agreement with test results than would a finer subdivision.

Another aspect of interest related to element size is the response for moments on the descending branch of the $M-\phi$ relationship. In an actual structure, displacements may be increased beyond the point at which maximum moment resistance (m_u, Fig. 4) has been reached at the critical base region. However, in a conventional first order sectional analysis, as well as in a standard finite element analysis with a very small element at the critical region, the end displacement can not be increased beyond this stage. This can be explained by considering the response to an attempted increase in end displacement. At the critical section with maximum moment, the moment would decrease along the descending $M-\phi$ branch with increasing curvature. Moments at all other sections would have to decrease correspondingly, but by unloading with decreasing curvatures from the ascending branch. Since a curvature increase at a single critical section, or over a very short element in the critical region, does not contribute to the displacement, the reduced curvatures over the remainder of the column would imply a reduced displacement, i.e., an obvious contradiction. However, using a larger element at the critical region than envisioned above, the curvature increase over the element may more than balance the reduced curvatures over the remaining elements. Thus, additional displacements, increasing with increasing element size may be predicted. These might be in better agreement with test results than those of a finer subdivision, but may create inaccuracies in the computed internal forces due to the larger element size.

The problem of choosing an element size that would give a reasonable quantitative estimate of the above phenomena for the general case, would be, like the question of the true plastic hinge length itself, quite difficult to determine without careful study of solutions for several selected element subdivisions. The above discussion emphasizes the fact, often overlooked in nonlinear finite element analyses, that the mesh size selected may have an important influence on the results obtained compared to those from a real physical model.

4. COMPARISON WITH TEST DATA

The applicability of the present procedure has been demonstrated by comparison to a variety of test results of reinforced and prestressed beams and columns subjected to both short time and time dependent load histories [1,6,5].

A summary is given below of one of these comparisons [5] involving a hinged, symmetrically reinforced concrete column, subjected to an eccentrically applied axial load history consisting of a sustained service load for 131 days, 1444 load repetitions and subsequent loading to failure in a stroke controlled test, Fig. 5. The column is one of a test series reported in [7,8].

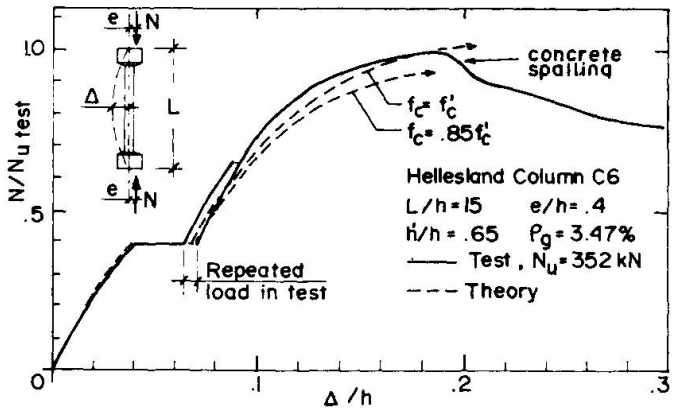

Fig. 5 Comparison with Test Data [7,8]

The material laws presently incorporated into the analysis do not account for effects on strength and strains of repeated loading. However, based on the above and other tests [9], it is believed that the relatively low number of repetitions and repeated load levels in the test may have had some, but only an insignificant, beneficial effect on stiffness and load capacity. Thus, a meaningful comparison can be obtained in this case in spite of the neglect of repeated loading in the analysis.

Column geometry and material data were as follows:

L = 1905 mm, $b \times h$ = 179 × 127.5 mm (average "as measured" in vicinity of midheight),

$A_s = A'_s$ = 396 mm^2 (1 #5 rebar in each corner),

h' = 82.6 mm, e = 50.8 mm, f'_c at initial (14 days) and final (145 days) loading 32.1 and 41.9 MPa respectively, f_y = 407 MPa,

E_{s1} = 211000 MPa (E_{s2} = 0, Fig. 3).

Over a length of 0.135L at column ends, the cross sections were enlarged to $b \times h$ = 229 × 406 mm.

Cylinder strength increases with time due to hydration, shrinkage (ε_{sh}), creep and effect on creep of age at loading (t'), as measured on plain concrete cylinders (152 × 304 mm), were approximated in the analysis as follows:

$$f'_c = f'_{c28} \cdot t/(4.32+0.845t); \quad f'_{c28} = 37.1 \text{ MPa}$$

$$\varepsilon_{sh} = 650 \cdot 10^{-6}(1 - e^{-t/60})$$

Creep: Eq. 2 with $c_u = 8.760 \cdot 10^{-5}\ (1.46 - 0.32 \log_{10} t')$ (per MPa)

$$a_1 = .386, \quad a_2 = .352, \quad a_3 = .262$$

The concrete σ-ε diagram used (Fig. 3) is defined by $E_{co} = 4735\sqrt{f_c}$ (MPa), $\varepsilon_o = 2f_c/E_{co}$, $\varepsilon_u = .0038$, $z = 79$ and $f_t = 0.5\sqrt{f_c}$. The structural concrete strength f_c is taken in terms of the time dependent cylinder strength as either 0.85 f'_c or 1.0 f'_c. The column, including the enlarged ends, was modelled using 8 elements for the half length. Each cross section was divided into 10 layers. The sustained load period was divided into 6 time intervals of increasingly larger duration.

Good agreement between test and theoretical load-deflection results can be noted, Fig. 5, with the better correspondence obtained with $f_c = 1.0\, f'_c$.

5. COLUMN DEFORMATION CAPACITIES

5.1 General

Controlled deformation and deformation capacity results from the analysis of several reinforced concrete columns with constant axial loads are presented below, and the effect on the results of important parameters are discussed.

The columns, representative of such as those in Fig. 1, are modelled as shown in Fig. 6. Apart from the controlled end deformations at the column top and shortening due to axial loading, the columns considered are fixed at both ends. This is achieved by assigning spring constants to the spring restraints (Fig. 6) that are several order of magnitudes larger than the rotational or translational column stiffness. External forces at the column top, required to produce a specified end rotation or displacement, are therefore a function of the spring constants alone.

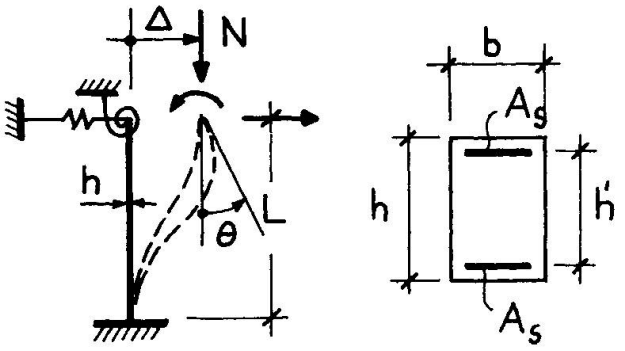

Fig. 6 Column Model and Cross Section

The columns all have constant, symmetrically reinforced cross sections, Fig. 6, with $h'/h = 0.85$. Cross sections are divided into 10 or 20 equal layers, with the finer layer division used for elements in the most strained regions of the column. Element lengths were chosen after careful study such that the pure flexural inelastic action was captured with reasonable accuracy.

While the results include both short and long term applications of controlled end displacements, end rotations are applied in a short term sense only.

Short term rotations and displacements are applied incrementally in 5 to 8 steps. Unless indicated otherwise the axial load is applied in the first step together with a small displacement or rotation. Long term displacements are applied incrementally over a period of 10,000 days (approx. 27 years) in two load increments at each time step as indicated in Fig. 7, where the time domain is divided into 8 intervals. Equivalent nonmechanical forces due to column creep are applied in one increment at each time step. Column shrinkage is not considered.

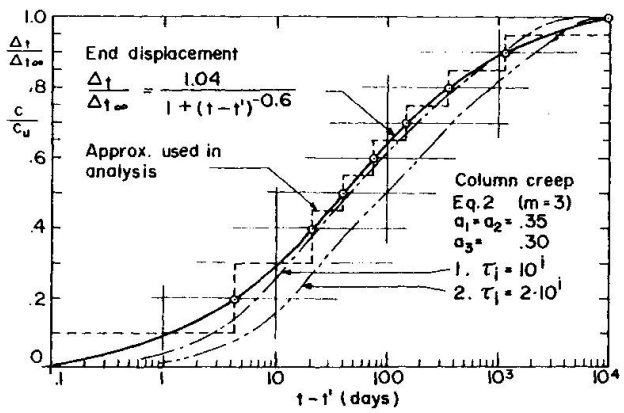

Fig. 7 Development of Time Dependent End Displacement and Column Creep with Time

Results presented below are based on creep curve "1", Fig. 7. Ultimate specific creep is taken as

$$c_u = 7.6 \cdot 10^{-5}\, (t'/t'_o)^{-0.118} \quad (MPa^{-1}) \quad (3)$$

with initial loading at $t_o' = 28$ days. This corresponds to a creep coefficient $\phi(t_o') = c_u E_{co} = 2.0$ for a concrete with $f_c = 25$ MPa and properties otherwise as given below. Only linear creep is considered.

Concrete strength and E-modulus is not assumed to increase with time, in order to be in line with common design practice. The constitutive stress strain relationships used, Fig. 3, are defined by

- $f_t = 0.1\, f_c'$, $\varepsilon_o = 0.0019$, $\varepsilon_u = 0.0038$ and $z = 79$

- $\varepsilon_{sy} = 0.00207$, $\varepsilon_{su} = 0.030$ and $E_{s2} = 0$.

Results are given in terms of the nondimensional axial load n, moment m and mechanical reinforcement ratios w and w';

$$n = N/f_c bh$$

$$m = M/f_c bh^2 \qquad (4)$$

$$w = w' = f_y A_s/f_c bh$$

Thus, within the constraints imposed by the assumed stress strain laws, the results are valid for any concrete (f_c) and steel strength (f_y).

Deformation capacities are limited by member failure caused by either primary material or section failure as maximum sectional moment resistance is reached, before or at a maximum concrete compressive strain of ε_u or steel strain of ε_{su} (does not govern), or by primary instability (buckling between column ends) due to nonlinear geometric effects at strains below the above limits.

5.2 Rotation and Displacement Results

Typical moment and maximum deflection (y_{max}) results versus controlled end rotations (θ) are shown in Fig. 8, and moment versus controlled end displacements in Fig. 9. Points at which rebars yield in compression (Y') or tension (Y) and where the concrete strain reaches ε_o (Fig. 3) are indicated on the figures. The reinforcement ratio in these figures ($w = 0.0828$) corresponds to a total steel percentage of approx. 1% for $f_c = 25$ MPa and $f_y = 400$ MPa.

Typical deflection and moment distributions along the length are indicated schematically in Fig. 10. Maximum moments (m_{max}) may occur at column ends, or, with increasing nonlinear geometric effects, at an increasing distance from column ends. Also shown (Fig. 10) is the additional deflection due to nonlinear geometric effects, computed as the difference in results ($y_2 - y_1$) of second and first order analyses for a given end rotation or end displacement. Essentially, these shapes correspond to the first and second Euler buckling mode for fixed ended columns with sway prevented. Results associated with controlled end displacements of initially straight columns, as in the present study, are anti-symmetric about midheight. For such cases it is sufficient to analyze one half of the column.

Some moment-deformation aspects, typical for slender columns, may be discussed with reference to the columns with end rotation in Fig. 8. The top moment m_t increases with increasing rotation θ until it reaches a maximum prior to column failure. This maximum moment, which would be the one of main interest in a strength analysis, is for the more slender column ($L/h = 45$) considerably smaller than the sectional moment resistance due to the nonlinear geometric effects.

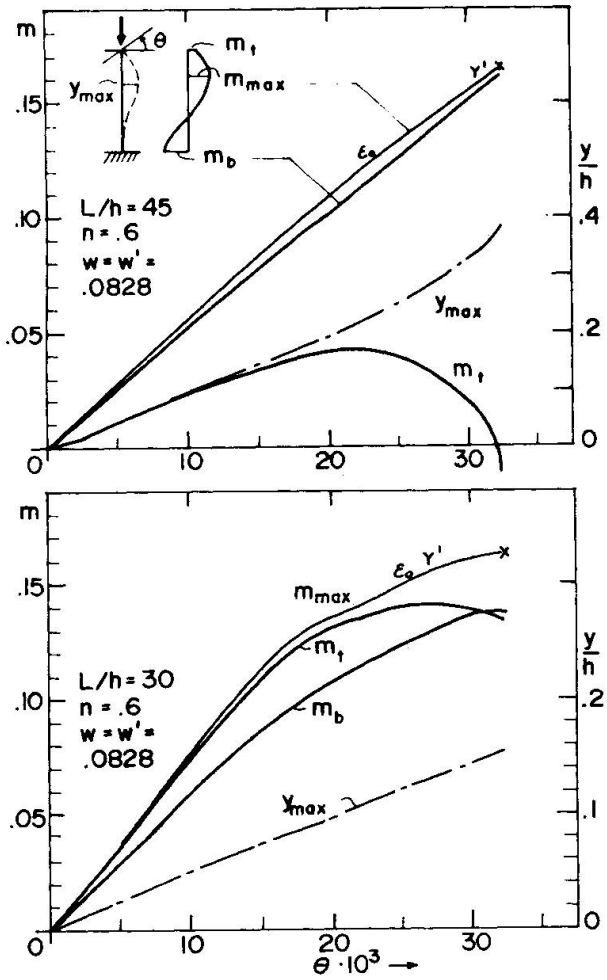

Fig. 8 Typical Moment versus Rotation Results

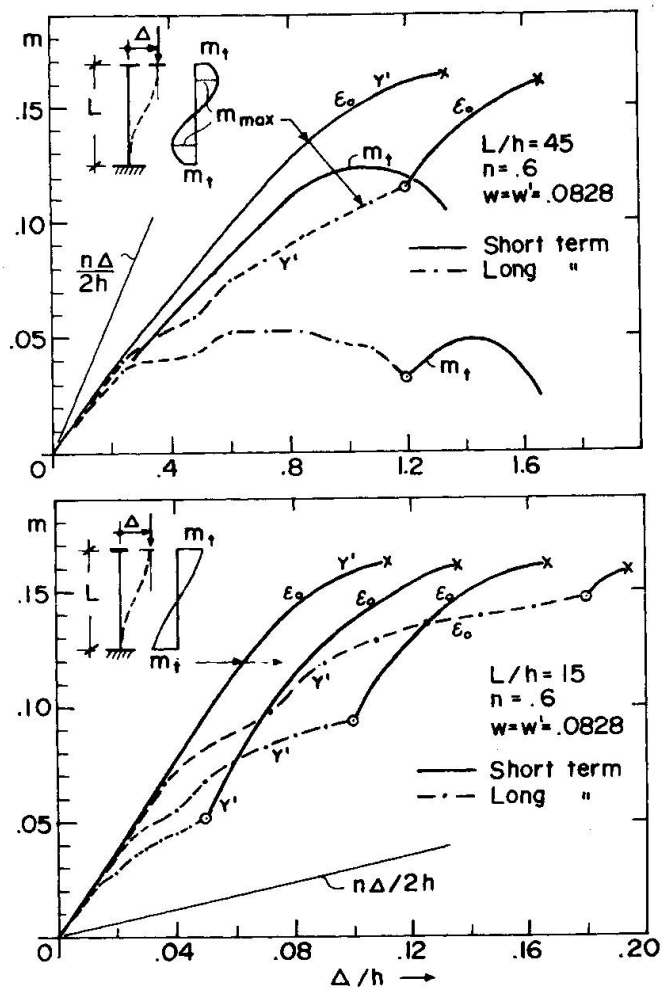

Fig. 9 Typical Moment versus Displacement Results

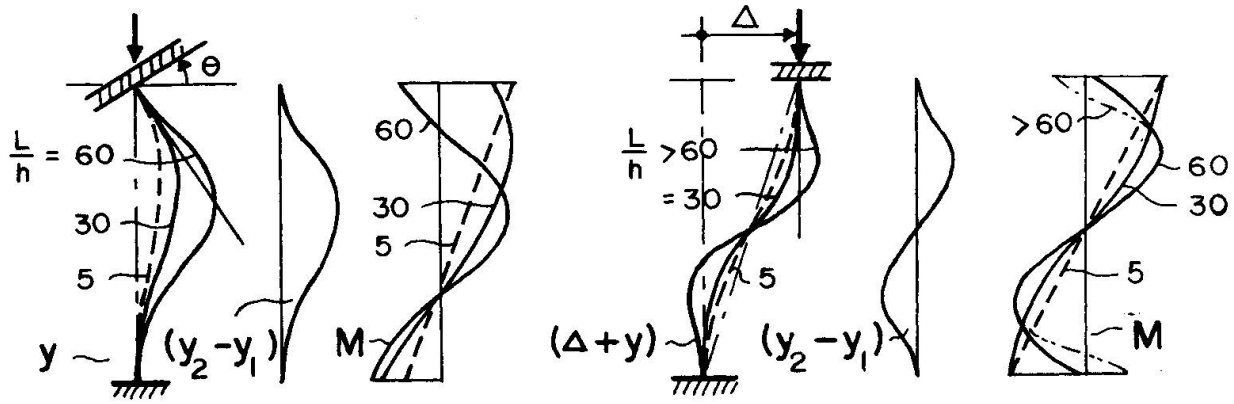

Fig. 10 Schematic Short Term Deflection and Moment Distributions at Failure (n~0.6; w~.08)

With further increase in θ, m_t decreases until at some point it may become zero and thereafter change direction. Thus, rather than resist the imposed rotation from this point on, the column needs moment support in order not to collapse. In an actual structure, this moment support must be provided by the girder. However, the column may still be able to carry axial loads and accommodate further imposed rotations, until material failure or buckling (between ends) occur.

Similar behaviour can be observed for columns with controlled end displacements. The lateral column resistance or support under increasing end displacements is given by the shear force V in the column,

$$V = \frac{2}{L}\left(m_t - \frac{N\Delta}{2}\right) \tag{5}$$

The second term in Eq. 5 is shown (nondimensionalized) in Fig. 9. For the column with L/h = 45 it is always larger than m_t. Consequently, this column needs lateral support from the onset of imposed displacements.

The slenderness or axial load at which a column needs moment or lateral support already at the onset of imposed deformations, can be determined from the usual Euler load expression. For this computation a stiffness (EI) corresponding to the tangent at the origin of the respective M-ϕ relationships should be used.

5.3 Short Term Deformation Capacities

Short term end rotation and end displacement capacities, θ_{uo} and Δ_{uo} respectively, obtained by increasing θ and Δ incrementally as shown in Figs. 8 and 9, are given in Fig. 11 for various slenderness ratios and two axial load levels that comprise load levels of practical interest. Points at which results have been calculated are indicated by circled values. The variation drawn in between these values is approximate only. Also shown are results from first order analyses which neglect geometric nonlinearities.

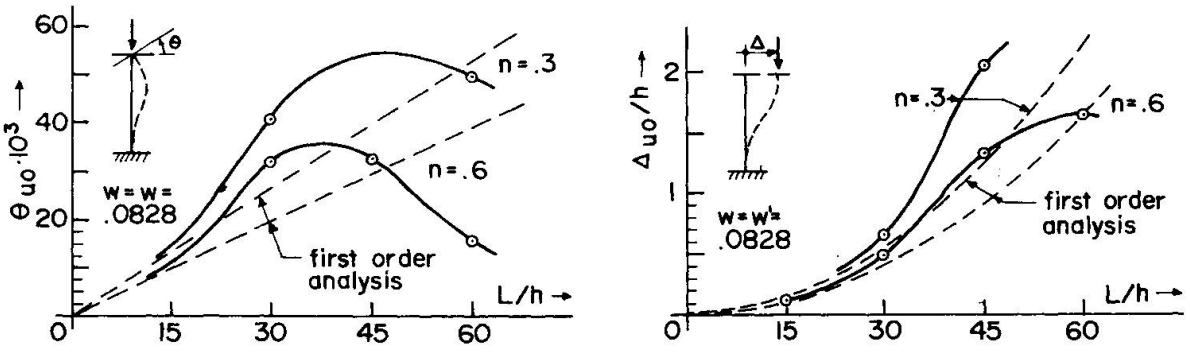

Fig. 11 Short Term Rotation and Displacement Capacities

Material failure was the primary cause of failure for columns subjected to controlled end rotations and n = 0.3 for all L/h ratios up to about 60. This was also the case for n = 0.6 for L/h values less than about 50. Thereafter, failure was by primary instability (buckling associated with rapid deflection increases between the column ends). Columns with controlled end displacements are less sensitive to nonlinear geometric effects due to the smaller "buckling" length, Fig. 10, and thus all failed by primary material failure. For n = 0.6 and L/h = 60, end moments were approximately zero at this point.

Conventional computation of moment-curvature curves and integration of curvatures based on linear moment distribution over the column length, gave results in good agreement with the first order computer results, Fig. 11 (broken lines). First order rotation and displacement capacities vary linearly and parabolically respectively w.r.t. the column slenderness for a given n and w,

$$\theta_{uo}/h = a\ L/h \tag{6}$$

$$\Delta_{uo}/h = b\ (L/h)^2 \tag{7}$$

where, for $w = 0.0828$, the following approximate constants were found for $n = 0.3$ and $n = 0.6$: $a = 0.880 \cdot 10^{-3}$ and $0.650 \cdot 10^{-3}$; $b = 0.625 \cdot 10^{-3}$ and $0.455 \cdot 10^{-3}$. These expressions may be used to compute deformation capacities for small L/h values where the geometric nonlinearity effect is negligible, Fig. 11.

For most L/h values of practical interest, the first order capacities are on the safe side. As long as maximum moment and failure is obtained at the column ends, the discrepancy between second and first order analysis results increases at an increasing rate with increasing slenderness due to the additional moments brought about by the geometric nonlinearity (axial load on deflections) in the second order solution. As maximum moments start forming at an increasing distance from column ends at larger slenderness values, and as end moments reduce, Fig. 10, this discrepancy gradually tapers off and may eventually change sign as seen in Fig. 11 as the second order curve crosses over the first order curve.

In a real structure columns will usually be subjected to both end rotations and end displacements. The effect on displacement capacities of a previously imposed end rotation; θ, applied simultaneously with the axial load, can be seen in Fig. 12. All values are given in terms of the short term (single action) capacities in Fig. 11 for the respective slendernesses. Of interest in Fig. 12 are also the first order results which are seen to be on the safe side.

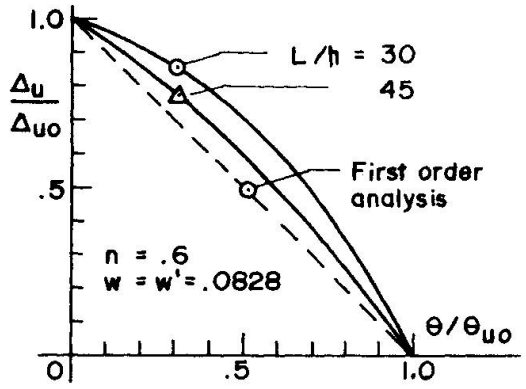

Fig. 12 Effect of Previously Imposed Rotation on Displacement Capacity

Short term deformation capacities appear to increase with increasing reinforcement, decreasing axial load, and, as seen in Fig. 12 with increasing slenderness ratios up to a certain point. Similar results have been found in other investigations for single action end displacements [4].

The flexural deformation capacity results computed above are on the safe side, in particular for shorter columns with insignificant nonlinear geometric effects. The additional deformation potential of such columns due to the spread of the inelastic zone caused by lateral tie or hoop confinement, longitudinal strain gradients, strain hardening of the steel, bond slip, inclined shear cracking, extended concrete crushing, etc., may be estimated for an actual column using procedures described in available code or code related publications, summarized in [10].

5.4 Time Dependent Effects

When end displacements are applied gradually over a period of time, creep in the column tends to relieve the development of internal column moments as seen, Fig. 9, when comparing moments obtained in a short term and long term (broken lines) application of the same end displacement. The dips in the long term moment curves are partly due to the discretization in time in the analysis, and partly, due to the differences in variation with time assumed for end displacement and specific creep (Fig. 7).

The effect of a given time dependent displacement on final displacement capacities, Δ_u, was obtained by incrementing the end displacement in a controlled short term application after the given total time dependent displacement $\Delta_{t\infty}$ had been attained. It is seen, Fig. 9a, that the magnitude of the total time dependent displacement $(\Delta_{t\infty})$, which is always applied over the same period of

time (27 years) and in the same manner (Fig. 7), may have a significant effect. Similar studies were carried out for other columns. Typical results for columns with relative high axial load levels, with most of the cross section in compression, and small reinforcement ratios are summarized in Fig. 13, which is non-dimensionalized in terms of short term capacities Δ_{uo} that can be obtained from figures such as 9 and 11b (second order).

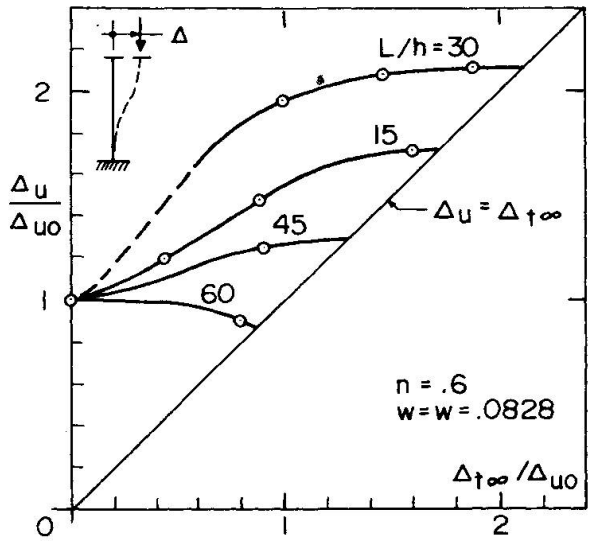

Fig. 13 Total Displacement Capacity versus Long Term Displacement

Figure 13 clearly shows the effect of an initial imposed long term displacement $\Delta_{t\infty}$ and slenderness ratio on the total displacement capacity Δ_u. For high slenderness ratios in combination with high axial loads and small reinforcement ratios, as in the present case for L/h = 60, large creep deflections measured from the chord through the column ends may cause premature failure through instability at end displacements less than Δ_{uo}. However, for small and intermediate slenderness ratios, and load levels and reinforcement ratios of practical interest, an increase in displacement capacity beyond Δ_{uo} will usually result when part of the displacement is applied gradually over a period of time.

The increase may not be as large as that shown in Fig. 13 for other n and w values. For example, by either reducing n in Fig. 13 to 0.3 or by increasing w to 0.25, increases of 41% and 50% respectively were found for $\Delta_{t\infty}/\Delta_{uo} = 0.77$ as compared to approximately 80% above, for L/h = 30.

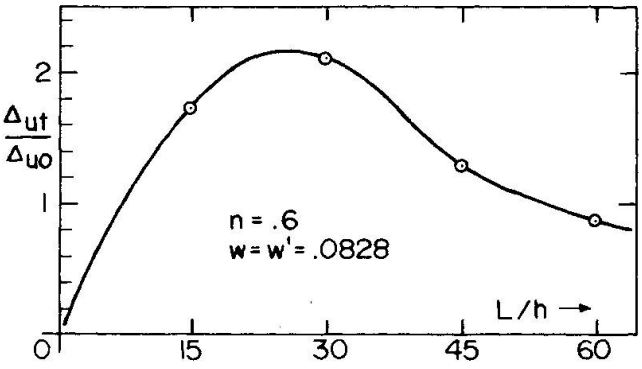

Fig. 14 Long Term Displacement Capacity versus Slenderness Ratio

Figure 14 shows the largest long term displacements that can be applied for a given slenderness for failure to take place just at the end of the time period considered. These values are given by the intersection of the curves in Fig. 13 and the 45° line in the same figure.

A non-exhaustive comparative study of the effects on displacement capacities of nonlinear creep, slower creep development with time (curve "2" in Fig. 7) and of replacing parts (about 40%) of the time dependent displacement ($\Delta_{t\infty}$) above with a short term initial displacement, was also carried out. The latter two factors do not appear to affect capacity results significantly. Nonlinear creep may increase total displacement capacities of shorter columns due to increased creep "relief", while slender columns with large geometric nonlinearity may be affected adversely. Similar results can be expected for larger creep values than that used in the present study (Eq. 3).

6. SUMMARY AND CONCLUSIONS

A study of reinforced concrete columns under imposed end rotations and displacements has been presented. Numerical solutions were obtained using a finite element computer program, PCFRAME, capable of performing nonlinear and time dependent analyses of reinforced and prestressed concrete frames. Choice of element subdivision, nonlinear geometric effects, initially applied rotations and time dependent displacements were found to have significant effects on total displacement capacities.

Additional nonlinear analytical studies are planned to develop sufficient data from which improved design recommendations may be made for reinforced concrete bridge columns under imposed deformations.

ACKNOWLEDGEMENTS

This research was partially sponsored by the National Science Foundation by Grant No. CME-7918057. Additional support was provided to the first author from the Royal Norwegian Council for Industrial and Scientific Research (NTNF), Janson's Legat and Dr. Ing. A. Aas-Jakobsen A/S. The Computer Center at the University of California, Berkeley, provided the facilities for the numerical work.

REFERENCES

1. KANG, Y.-J., and SCORDELIS, A. C., "Nonlinear Analysis of Prestressed Concrete Frames," Journal of the Structural Division, ASCE, Vol. 106, No. ST2, Febr. 1980.

2. GHALI, A., DILGER, W., and NEVILLE, A. M., "Time-Dependent Forces Induced by Settlement of Supports in Continuous Reinforced Concrete Beams," ACI Journal, Nov. 1969.

3. BISHARA, A. G., and JANG, S.-Z., "Settlement-Induced Forces in Concrete Bridges," Journal of the Structural Division, ASCE, Vol. 106, No. ST7, July 1980.

4. GRENACHER, M., "Einfluss von Verschiebungen und verschiedenen Lagerungen auf das Traqverhalten von Stahlbetonstützen," Bericht Nr. 61, Institut für Baustatik und Konstruktion, ETH, Zürich, Febr. 1976.

5. HELLESLAND, J., "Nonlinear, Time Dependent Analysis of R. C. Bridge Columns under Imposed Deformations and Lateral Loads," UC-SESM Report (in preparation), Univ. of California, Berkeley.

6. KANG, Y.-J., "Nonlinear Geometric, Material and Time Dependent Analysis of Reinforced and Prestressed Concrete Frames," UC-SESM Report No. 77-1, Univ. of California, Berkeley, Jan. 1977.

7. HELLESLAND, J., "A Study into the Sustained and Cyclic Load Behaviour of Reinforced Concrete Columns," Ph.D. Dissertation, Dept. of Civil Engineering, Univ. of Waterloo, Waterloo, Ont., Canada, Aug. 1970.

8. HELLESLAND, J., and GREEN, R., "Sustained and Cyclic Loading of Concrete Columns," Journal of the Structural Division, ASCE, V. 97, No. ST4, Apr. 1971.

9. GREEN, R., and HELLESLAND, J., "Repeated Loading Tests of Reinforced Concrete Columns," ACI Publication, SP-50, 1975.

10. PARK, R., and PAULAY, T., "Reinforced Concrete Structures," John Wiley & Sons, 1975.

NOTATIONS

b - width of concrete section
h - depth of concrete section
h' - distance between compression and tension steel
L - column length
A_s - tensile steel area
A'_s - compression steel area
f_c - structural concrete compressive strength
f'_c - cylinder concrete compressive strength
f_t - structural concrete tensile strength
f_y - yield stress of reinforcing steel
E_{s1} - initial elastic modulus of reinforcing steel
E_{s2} - post yield elastic modulus of reinforcing steel

ε - total strain
ε_c - mechanical (instantaneous) concrete strain
ε_{cc} - concrete creep strain
ε_{sh} - concrete shrinkage strain
ε_o - concrete strain at maximum stress
ε_u - concrete crushing strain
ε_y - steel strain at yield
ε_{su} - steel strain at fracture

Δ - imposed (controlled) end displacement
Δ_u - end displacement capacity
Δ_{uo} - single action short term end displacement capacity
Δ_{ut} - single action long term end displacement capacity
θ - imposed (controlled) end rotation
θ_{uo} - single action end rotation capacity
$\Delta_{t\infty}$ - long term end displacement applied gradually over a period of approximately 27 years

Leere Seite
Blank page
Page vide